INSTITUTE OF PHYSICS PUBLISHING PHYSICS IN MEDICINE AND BIOLOGY

Phys. Med. Biol. **48** (2003) 3851–3863 PII: S0031-9155(03)62529-7

Dual photon absorptiometry using a gadolinium-153 source applied to measure equine bone mineral content

Alessandro Moure[1], **Peter Reichmann**[2] **and Humberto Remigio Gamba**[3]

[1] National Scientific and Technological Development Council, Ministry of Science and Technology, SEPN 509, Bloco A, Sala 204, 70750-901 Brasília, DF, Brazil
[2] Department of Veterinary Clinical Medicine, Agricultural Science Centre/Londrina State University, CP 6001, 86051-990 Londrina, PR, Brazil
[3] Centro Federal de Educação Tecnológica do Paraná, Post-Graduate Programme in Electrical Engineering and Applied Computer Science, Av. 7 de setembro 3165, 80230-901 Curitiba, PR, Brazil

E-mail: amoure@cnpq.br, reichman@uel.br and humberto@cefetpr.br

Received 23 April 2003, in final form 24 September 2003
Published 7 November 2003
Online at stacks.iop.org/PMB/48/3851

Abstract

The application of the dual photon absorptiometry (DPA) technique, using gadolinium-153 as the photon source, to evaluate the bone mineral density (BMD) of the third metacarpal bone of horses is presented. The radiation detector was implemented with a NaI(TI) scintillator coupled to a 14 stage photomultiplier. A modular mechanical system allows the position of the prototype to be adjusted in relation to the animal. A moveable carrier makes it possible to scan the third metacarpal with a velocity adjustable between 1 and 12 mm s^{-1}, in steps of 1 mm s^{-1}, for a total distance of 250 mm. The prototype was evaluated with a phantom of the third metacarpal bone made of perspex and aluminium, and *in vitro* with a transverse slice of the third metacarpal bone of a horse. The tests showed that the prototype has an accuracy and precision of, approximately, 10% and 6%, respectively, for a 6 s acquisition time. Preliminary studies carried out in three foals from birth to one year of age indicated that the prototype is well suited to *in vivo* and *in situ* analysis of the BMD of the third metacarpal bones of horses, making it possible to evaluate the changes of BMD levels on a monthly basis. Also, results indicated an exponential behaviour of the BMD curve during the first year of life of the studied horses.

1. Introduction

The bone mineral density (BMD) is a parameter that can be used by veterinarians to diagnose and follow up many diseases. In horses, the determination of the BMD has been used in

academic research to assess the influence of age (Lawrence *et al* 1994) and environmental factors such as diet, weaning (Hoffman *et al* 1999), training (Porr *et al* 1997, Nielsen *et al* 1997), stall confinement (Bell *et al* 2001) and limb immobilization (Buckingham and Jeffcott 1991) on skeletal development and maturity. The application of BMD determination in veterinary medicine has been limited by the lack of appropriate equipment to be used with animals.

For the sequential and non-invasive determination of BMD *in vivo* in horses, the most frequently used techniques are radiographic photo-densitometry, with results expressed in radiographic bone aluminium equivalent, and ultrasound transmission velocity through the bone. Techniques for *in vitro* measurements of bone characteristics also include single photon absorptiometry (SPA) and dual photon absorptiometry (DPA) and computed tomography. Ultrasound transmission velocity is an indirect means for BMD determination, while photon absorptiometry directly measures BMD and is reported to be more sensitive than radiographic photo-densitometry for this kind of analysis. SPA uses a monoenergetic americium (^{241}Am) source and results can be expressed in g cm^{-2}. The disadvantage is the need for a soft tissue equivalent surrounding the limb with the bone to be examined (Jeffcott *et al* 1988). DPA can be applied using a bienergetic gadolinium-153 source or dual-energy x-ray absorptiometry (DXA) (Grier *et al* 1996, McClure *et al* 2001). There is no need for a soft tissue equivalent and the results are expressed in g cm^{-2} (Jeffcott *et al* 1988). While SPA has had some application *in vivo*, DPA and computed tomography have, due to equipment limitations, so far only been used for studies *in vitro* with excised bone.

In this paper, we have investigated the DPA technique applied to measure equine BMD using gadolinium-153 as the photon source. For this we have produced a prototype of a BMD quantifier. The bench tests were performed with a phantom used to simulate bone and soft tissues. The *in vitro* tests were made with an excised equine third metacarpal (MCIII). We also tested the DPA technique *in vivo* and *in situ* during a one year period in which we carried out studies in three foals during their first year of life.

2. Materials and methods

2.1. Selected region to measure the BMD in horses

There are two types of bone tissue: trabecular and cortical. In general, the bones are composed of a combination of these two types of tissue. Ideally, the BMD assessment should be done in regions where there is only one type of tissue. It was demonstrated that changes in the BMD of trabecular bone, due to disease for example, occur eight times faster than in cortical tissue (Ostlere and Gold 1991). Therefore, the trabecular tissue is best indicated to detect abnormal conditions of the skeletal system (Jeffcott *et al* 1988).

Unfortunately, in horses, bones composed predominantly of trabecular tissue are not easily accessed (Scotti and Jeffcott 1988). On the other hand, bones composed essentially of cortical tissue, such as the MCIII, are easily accessed by DPA (Grier *et al* 1996, Jeffcott *et al* 1988, Piotrowski *et al* 1983). Also the mid portion of the MCIII has a very well-defined geometry and it is easily located by anatomical inspection, which makes the repetitive scan reproducible. Therefore, the selected region to measure the BMD was the mid portion of the MCIII (figure 1).

2.2. Dual photon absorptiometry technique used to measure the BMD

The technique used to measure the BMD is bienergetic gamma-ray absorptiometry. This technique is based on the Beer–Lambert–Bouguer law (Willard *et al* 1988, Njeh *et al* 1999).

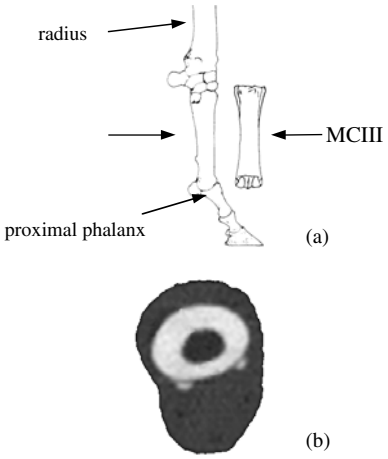

Figure 1. (a) Sketch of the MCIII of a horse (Piotrowski *et al* 1983). The absence of other superposed bone structures and its cylindrical geometry makes the BMD measurement simpler. (b) Tomographic slice of the middle region of the MCIII (resolution 256 × 256 pixels and 256 grey scale) (Batista 2000). The tomographic image shows that the MCIII is mainly made of bone (brighter region) and soft tissues (dark region).

Equation (1) gives the bone mineral thickness considering a beam with photons with two different energies and a sample composed of two different materials (Krølner and Nielsen 1985),

$$x_b = \frac{\mu_{t,1}\ln(I_{1,2}/I_{0,2}) - \mu_{t,2}\ln(I_{1,1}/I_{0,1})}{\mu_{b,2}\mu_{t,1} - \mu_{b,1}\mu_{t,2}} \quad \text{(cm)} \tag{1}$$

where

- x_b is the bone mineral thickness in centimetres at the point where the beam crosses the bone,
- $\mu_{t,1}$ is the linear attenuation coefficient of soft tissues for the photons with energy E_1,
- $\mu_{t,2}$ is the linear attenuation coefficient of soft tissues for the photons with energy E_2,
- $\mu_{b,1}$ is the linear attenuation coefficient of bone tissue for the photons with energy E_1,
- $\mu_{b,2}$ is the linear attenuation coefficient of bone tissue for the photons with energy E_2,
- $I_{0,1}$ is the intensity of the photon beam with energy E_1 that is incident to the sample,
- $I_{0,2}$ is the intensity of the photon beam with energy E_2 that is incident in the sample,
- $I_{1,1}$ is the intensity of the photon beam with energy E_1 after crossing the sample,
- and $I_{1,2}$ is the intensity of the photon beam with energy E_2 after crossing the sample.

Once the bone thickness, x_b, is measured, the BMD in g cm^{-2} is determined using equation (2),

$$\text{BMD} = \frac{\rho_b\left(\sum_0^n x_{b,n}\,\Delta\right)}{\text{bw}} \quad (\text{g cm}^{-2}) \tag{2}$$

where ρ_b is the bone density (Siemon *et al* 1974), bw is the bone width, n is the number of measuring points within the bone width and Δ is the sample interval, which in our experiments was set to 2 mm.

It is interesting to point out that even though soft tissues surrounding the MCIII comprise many different materials (e.g. muscle, skin, etc) the attenuation coefficients for all these materials are very similar. Thus a single value of attenuation coefficient can be used to represent it in equation (1) (Hubbel and Seltzer 1995).

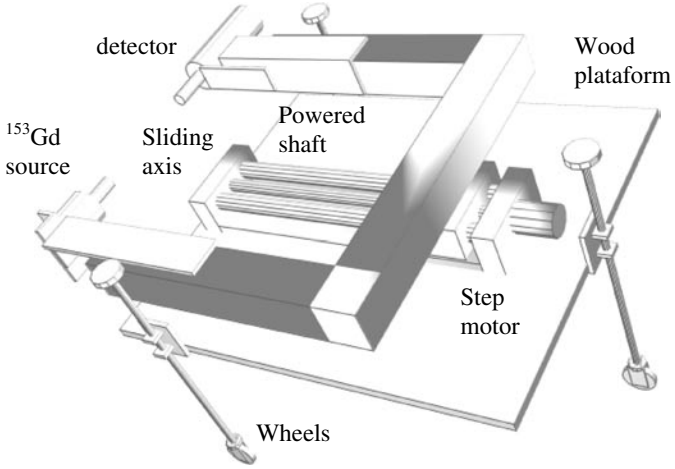

Figure 2. Sketch of the components of the mechanical system built to investigate the application of the DPA technique to measure equine BMD in the MCIII where it is possible to see: the fixation system for the ^{153}Gd source and the photon detector; the aluminium arms used to keep the photon beam and the detector aligned; the moving system for the aluminium arm made by SINCRO S.A. and the adjustable platform used for positioning of the prototype at the height of the middle region of the MCIII.

2.3. Photon source and beam geometry

A gadolinium isotope, ^{153}Gd, was used as a photon source, with an initial activity of 37 GBq (1 Ci). Gadolinium-153 has two characteristic emissions at 44 and 100 keV that are adequate to study organic tissues (Bushong 1993).

There are two collimators made of lead, one attached to the photon source, with an aperture of 2 mm, and another attached to the photon detector, with an aperture of 3 mm. The collimator diameters were calculated to avoid scattered photons for a fixed distance between the source and the detector of 250 mm. Sorenson and Cameron (1967) used the same collimator apertures in their system to measure bone mineral content in humans. Both collimators are 65 mm in length.

2.4. Mechanical system

The mechanical system is responsible for the positioning of the equipment and linear scanning of the MCIII. Figure 2 shows a sketch of the main components of the mechanical system. Basically, it is made of a C-shaped aluminium support of 1 mm thickness and dimensions of 45 cm $\times$ 40 cm $\times$ 45 cm, where the source and the detector are fixed at their extremities with an 'L' profile aluminium of 1 mm thickness. The C back is then fixed on a sliding table system controlled by a step motor. This design of the mechanical system allows data to be acquired when the system is moving in both directions, therefore for each cycle of movement two sets of data are acquired.

The scanning velocity is adjustable between 1 and 12 mm s^{-1}, with steps of 1 mm s^{-1}, for a total distance of 250 mm. The whole system is then mounted on a wood platform with free wheels. The height of the platform is adjustable between 100 and 450 mm.

It is possible to adjust the source and detector positions and photon beam alignment. The detector and source move in the horizontal and vertical axis, respectively. The alignment is made with the help of a laser emitter placed in the detector's holder.

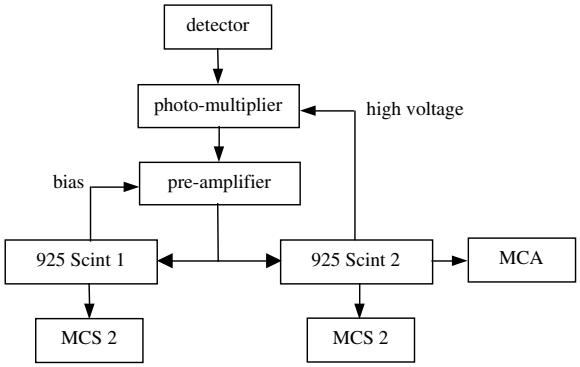

Figure 3. Block diagram of the electronic system used for the data acquisition.

2.5. Electronic acquisition and data processing system

Figure 3 shows a block diagram of the electronic system used to count the photons during the MCIII scanning. The system is made of a NaI(TI) scintillator coupled with a 14 stage photomultiplier (EG&G Ortec) connected to a pre-amplifier (E&G Ortec 276) and two amplifiers/voltage source/monochannel (EG&G Ortec 925 Scint). The data are acquired with two PC cards EG&G MCS (multi-channel scaler) 913, one for each characteristic energy of the source (44 and 100 keV). The EG&G MCA (multi-channel analyser) 919 card allows the operator to visualize the gadolinium-153 spectrum, adjust the gain of the amplifiers and the position and width of the monochannel windows. A C++ program was written to process the data acquired with a microcomputer. To derive the BMD from the counting data acquired by the MCS cards the program calculates the bone width (equation (1)) and the average BMD for the scans (equation (2)). The implementation program did not take into account any spillover correction for the 100 keV scattered photons that appear in the 40 keV counting window.

The number of measurement points for the mid portion of the MCIII ranged from 15 to 30, depending on the width of the bone, and each point is centre-to-centre 2 mm apart. Since the half-life of gadolinium-153 is 241 days, the counting rate changes during the experiment, thus the minimum counting was adjusted to at least 250 photons per data point. The typical counting rate per data point, with a speed of 10 mm s^{-1}, was at least 10 000 counts per second for the 44 keV photons.

2.6. Gold standard (GS) of aluminium used to control the data quality

A block of aluminium of 38 mm length by 38 mm width and 12.8 mm thickness was fixed near to the gadolinium-153 source, figure 6. Thus, all the MCIII scanning dataset also has the photon attenuation due to the aluminium block. Since the attenuation of this aluminium standard is constant, it can be used to verify the calibration of the monochannel windows and control the data quality. Since experiments were performed in the course of a year, under different weather conditions, on a farm without any environmental control, the performance of the detecting system had to be monitored.

2.7. Bench and in vitro tests with the prototype

Figure 4(a) shows the phantom of the MCIII constructed to perform the bench tests. The bone structure was simulated with a cylinder of aluminium of 25 mm diameter and 10 mm height.

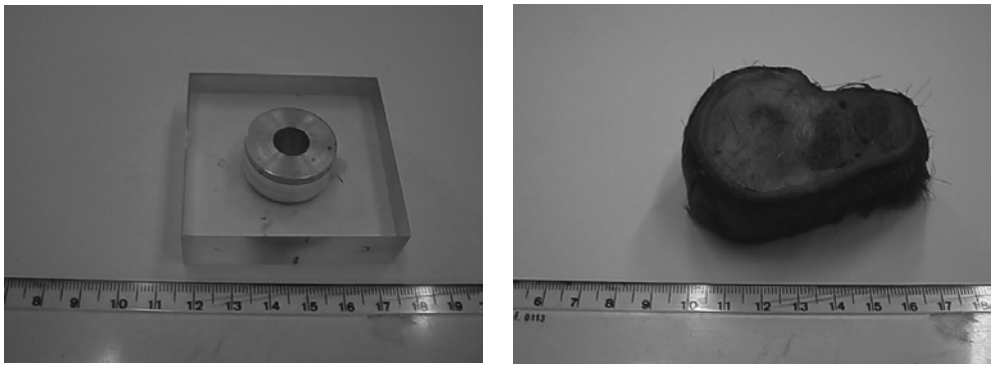

(a) (b)

Figure 4. (a) Picture of the phantom used to simulate an equine MCIII. The aluminium cylinder with a hole in its centre and the square perspex simulate the bone and the soft tissues, respectively. (b) Excised slice of the mid portion of an equine MCIII.

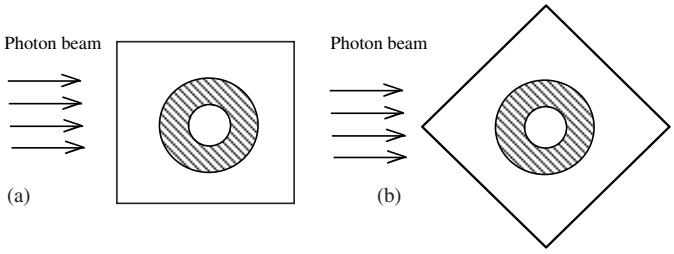

Figure 5. Sketch of the two photon beam incidences on the phantom shown in figure 4(a) during the *in vitro* tests. (a) First incidence, normal to the side of the square, less absorption by the perspex. (b) Second incidence, oblique to the square side, greater absorption by the perspex.

Table 1. Mass attenuation coefficient, μ/ρ, and density, ρ.

	ρ (g cm^{-3})	μ/ρ at 40 keV (cm^2 g^{-1})	μ/ρ at 100 keV (cm^2 g^{-1})
Perspex	1.190	0.2350	0.1641
Aluminium	2.699	0.5685	0.1704
Soft tissue (muscle, fat, skin, etc)	1.060	0.2688	0.1693
Bone mineral	3.18	0.6655	0.1855

The bone marrow cavity was simulated with a 10 mm diameter hole along the cylinder axis, filled with air. The soft tissues that cover the mineral bone were simulated with a 60 mm square block of perspex. Perspex and aluminium have absorption coefficients similar to soft and bone tissues, table 1. The prototype was also tested *in vitro* with an excised transverse slice of 20 mm thickness of an equine MCIII, figure 4(b). The *in vitro* data were collected on the same day the MCIII was excised and it had not received any treatment.

In the *in vitro* tests 20 and 10 scannings were performed with the phantom and the MCIII slice, respectively. As illustrated in figure 5, two experiments were made with the model: first with the beam incidence normal to the side of the square, resulting in minimum absorption by

the perspex; second with the beam incidence oblique to the square side, resulting in maximum absorption by the perspex. In both cases the beam incidence in the phantom was perpendicular to the cylinder axis. This procedure made it possible to evaluate the influence of the perspex thickness on the value of the aluminium mineral content (AlMC) measured in the experiment. The beam incidence in the sample was dorso-palmar, e.g., the sample was in the same position as it would be in the case of an *in vivo* experiment performed on the mid portion of a horse MCIII and the beam incidence on it was from the front to the back of the foal and the scanning movement was lateral, e.g. from the outside to the inside of the foal. Both the sample and the phantom were immersed in the air during their assessment.

During the *in vitro* experiments, using the MCA board (figure 3), the monochannels were adjusted to peaks at 44 keV and 100 keV. The scanning velocity was set to 10 mm s^{-1} and data were sampled every 2 mm. The scanning velocity and data sample were set as in the *in vivo* experiment, e.g., considering the limiting acquisition time of 6 s.

2.8. In vivo tests with the prototype

The *in vivo* and *in situ* tests were performed at a breeding farm. The BMD of three foals was measured during their first year of life. The examinations were performed weekly during the first month of life and during the month after weaning, otherwise monthly measurements were made.

A total of three foals were studied over 52 weeks. In order to improve the statistics four measurements were taken at the mid portion of the MCIII at each examination. The scanning velocity was 10 mm s^{-1} and the sample interval was adjusted to 2 mm. The short time necessary for one bone scan to be done made it possible to examine foals soon after birth, where one person kept the foal standing still and another person positioned the densitometer according to the height of the mid portion of the MCIII. The beam incidence in the MCIII was dorso-palmar, e.g., the beam incidence in the MCIII was from the front to the back of the foal and the scanning movement was lateral, e.g. from the outside to the inside of the foal.

2.9. Attenuation coefficients

The values of the mass attenuation coefficient, μ/ρ, and density, ρ, used in this work to calculate the AlMC and BMD are shown in table 1 and were obtained from Hubbell and Seltzer (1995). The density of pure bone mineral or microscopic density was obtained from Gong *et al* (1964).

3. Results

Figure 6 shows a picture of the prototype. For each photon beam incidence in the phantom (figure 5) ten measurements were made. The AlMC and BMD were obtained by equations (1) and (2) with the values of $\mu_{t,1}$, $\mu_{t,2}$, $\mu_{b,1}$, $\mu_{b,2}$ and ρ_b adjusted for perspex and aluminium, in the case of the phantom, and for soft tissues and bone, in the case of the excised transverse bone slice.

3.1. MCIII phantom results

Table 2 presents the ten values measured in each experiment, figure 5, performed with the MCIII phantom, figure 4. The AlMC was derived from equation (2), using the cylinder

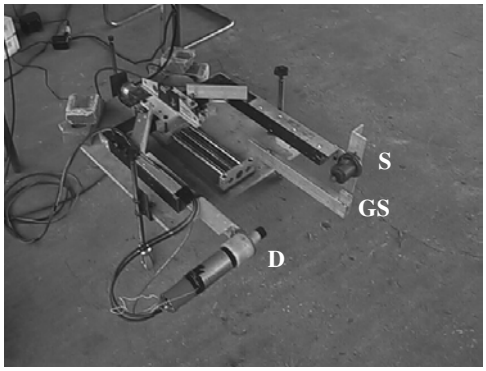

Figure 6. Picture of the prototype showing the gadolinium source and the photomultiplier detector. To protect the animal and the electronic components against a horse kick, since it may not like the presence of the prototype, during the examination both photon source and detector were covered with high density foam to prevent injuries to the horses. D, detector; S, ^{153}Gd source; GS, gold standard.

Table 2. Aluminium mineral content (AlMC) values measured with the MCIII phantom shown in figure 4(b). The photon beam incidences are illustrated in figure 5. σ is the standard deviation. All values are in g cm^{-2}.

	Normal beam incidence		Oblique beam incidence	
Experiment	GS AlMC	AlMC	GS AlMC	AlMC
1	3.40	3.84	3.38	3.92
2	3.40	4.13	3.42	3.84
3	3.39	3.93	3.40	3.56
4	3.42	4.07	3.43	3.97
5	3.39	3.95	3.41	4.11
6	3.41	4.13	3.41	3.92
7	3.36	3.89	3.38	3.82
8	3.40	4.05	3.40	4.02
9	3.41	3.94	3.39	3.92
10	3.37	3.73	3.40	3.80
Average	3.40 ($\sigma = 0.02$)	3.97 ($\sigma = 0.12$)	3.40 ($\sigma = 0.02$)	3.89 ($\sigma = 0.14$)

diameter x_b determined by equation (1) and the beam intensities measured with the prototype, figure 6.

The average of the ten measured values for the AlMC was 3.97 g cm^{-2} with a coefficient of variation of 3.1% and 3.89 g cm^{-2} with a coefficient of variation of 3.6% for the normal and oblique beam incidence, respectively. The cylinder diameter is 25 mm and the hole in its centre is 10 mm. The theoretical AlMC is the product of the area of the aluminium ring, 4.11 cm^2, by the aluminium density, 2.677 g cm^{-2}, divided by the external ring diameter, 2.5 cm. The theoretical AlMC is 4.44 g cm^{-2}. Thus, the accuracy of the *in vitro* measurements was 10.5% and 12.3% for normal and oblique beam incidence, respectively.

Table 2 also presents the values of the AlMC for the GS, which is fixed near to the Gd source, measured in each experiment performed with the MCIII phantom. Note that the average of the ten values measured in both experiments was 3.40 g cm^{-2} with a coefficient of variance of 0.6%. The expected theoretical AlMC value for the GS was calculated by multiplying the aluminium density, 2.699 g cm^{-3} (table 1), by the GS transverse section area

Table 3. BMD values measured in the *in vitro* experiment with the excised MCIII shown in figure 4(b). σ is the standard deviation.

Experiment	Bone mineral width (cm)	BMD (g cm^{-2})
1	3.6	2.58
2	3.6	2.58
3	3.6	2.81
4	3.6	2.54
5	3.6	2.72
6	3.6	2.78
7	3.6	2.74
8	3.6	2.50
9	3.6	2.57
10	3.6	2.70
	Average	2.65 ($\sigma = 0.10$)

(3.8 cm $\times$ 1.28 cm) and divided by its length, 3.8 cm, which gives 3.45 g cm^{-2}. Thus, the accuracy in the measurement of the AlMC of the GS was 1.15%.

Comparing these three coefficients of variance (3.1%, 3.6% and 0.6%) it is reasonable to expect that the DPA prototype with the Gd source, for a 6 s period acquisition and scanning velocity of 10 mm s^{-1}, is capable of measuring the BMD with a coefficient of variance lower than 4% provided the photon count rate is roughly the same.

The main difference between the measured and expected values for the MCIII phantom is the photon counting level used to calculate the object thickness. To minimize the acquisition time we have minimized the sample exposition, thus implying low photon counting. According to Cameron *et al* (1968) the precision and accuracy of the measured data used to calculate the object thickness is directly dependent on the photon counting levels.

Another source of error in the measurements comes from the fact that the ^{153}Gd source emits nine different gamma photons. Five of them have relevant probabilities: three in the 44 keV region (40.90, 41.54 and 47.00 keV) and the other two in the 100 keV region (97.43 and 103.18 keV). The detection system does not have enough resolution in energy to differentiate these photons and thus they are perceived as two peaks, as required by Beer's law. The problem is that the ambient temperature affects the energy resolution of the detection system, and the width of the peak gets wider at higher temperatures. Thus, during the experiment the performance of the detection system changes and these changes are detected through the analysis of the AlMC of the gold standard. When the value of the AlMC of the GS was higher than two standard deviations, the width of the windows was recalibrated, with the help of the MCA board.

Others sources of errors are (1) the gamma-ray beam which is divergent once it leaves the collimator, (2) the theoretical AlMC is calculated considering the exact ring area while in the experiment the measurements are taken in steps of 2 mm by continuously moving the source and the detector, (3) the beam diameter can lead to an error of up to $\pm$2 mm, since it is difficult to precisely determine the point where the phantom starts and finishes. All these sources affect the measurement of bw, equation (2), which propagates to the BMD measurement.

3.2. In vitro results obtained with the excised equine MAD

Table 3 presents the values of the BMD measured in the *in vitro* experiment. The average of the BMD values measured *in vitro* was 2.65 g cm^{-2} and the standard deviation was 0.10 g cm^{-2}. The coefficient of variance is 3.8%, which is slight worse than the 3.6% obtained

Table 4. Average and standard deviation (σ) of four measurements of the BMD values in the three foals during the course of 52 weeks. All values are in g cm^{-2}.

Age	Horse 1		Horse 2		Horse 3			
(weeks)	Average	σ	Average	σ	Average	σ	Average	σ
0	**1.31**	**0.0197**	**1.16**	**0.1480**	**1.24**	**0.0750**	**1.24**	**0.0613**
1	**1.43**	**0.0840**	**1.47**	**0.0478**	**1.35**	**0.0346**	**1.42**	**0.0499**
2	1.30	0.0451	1.49	0.0800	–	–	1.40	–
3	–	–	1.59	0.0342	1.51	0.0044	1.55	–
4	1.43	0.0543	–	–	1.57	0.0167	1.50	–
8	**1.73**	**0.0441**	**1.88**	**0.0578**	**1.99**	**0.0886**	**1.87**	**0.1066**
11	2.26	0.0142	2.12	0.0724	–	–	2.19	–
12	–	–	–	–	2.22	0.1432	2.22	–
15	2.37	0.0859	2.35	0.0997	–	–	2.36	–
16	–	–	–	–	2.32	0.1005	2.32	–
19	2.44	0.0925	–	–	–	–	2.44	–
20	–	–	2.48	0.0830	–	–	2.48	–
21	–	–	2.50	0.1151	2.40	0.1717	2.45	–
22	**2.50**	**0.1219**	**2.57**	**0.1667**	**2.50**	**0.0784**	**2.52**	**0.0330**
23	**2.56**	**0.0864**	**2.49**	**0.0555**	**2.52**	**0.0563**	**2.52**	**0.0287**
24	2.60	0.1074	–	–	2.51	0.0483	2.56	–
25	2.57	0.0466	–	–	–	–	2.57	–
27	2.73	0.0370	2.68	0.0471	–	–	2.71	–
31	–	–	2.52	0.0510	–	–	2.52	–
32	–	–	–	–	2.88	0.1322	2.88	–
34	–	–	2.73	0.1069	–	–	2.73	–
35	2.83	0.0218	–	–	–	–	2.83	–
36	–	–	–	–	2.87	0.0533	2.87	–
39	**2.80**	**0.0173**	**2.75**	**0.1331**	**2.75**	**0.1331**	**2.77**	**0.0236**
43	**2.94**	**0.0946**	**2.76**	**0.1254**	**2.76**	**0.1254**	**2.82**	**0.0849**
47	**2.94**	**0.1616**	**2.83**	**0.0561**	**2.83**	**0.0561**	**2.87**	**0.0519**
51	3.04	0.0743	–	–	–	–	3.04	–
55	3.02	0.0313	–	–	–	–	3.02	–
59	3.08	0.0829	–	–	–	–	3.08	–
		$\sigma = 0.0385$		$\sigma = 0.0386$		$\sigma = 0.0468$	Reproducibility = 0.0550	
				Repeatability = 0.0413				

with the MCIII phantom. Table 3 also presents the excised MCIII width measured with the prototype, which was used to determine the BMD, equation (2).

The *in vitro* BMD values measured with our prototype are very similar to those published by other authors (Jeffcott *et al* 1986, Tomioka *et al* 1985). The standard deviation of the data measured with the slice of an equine MCIII is practically the same of that measured with the MCIII phantom.

3.3. Results in vivo

Table 4 presents the BMD values measured *in vivo* and *in situ*. The BMD values for horses 1, 2 and 3 in this table are the averages of four sequential measurements performed with each foal. Sometimes, it was not possible to measure the BMD in the same week for all three horses, that is why some values are not shown in table 4. To determine the experiment's reproducibility we have selected only those BMD values that were taken in the three foals at the same age. The average and the standard deviation of the values measured in the three horses are also presented in table 4. With the exception of the BMD values of the third week, all other

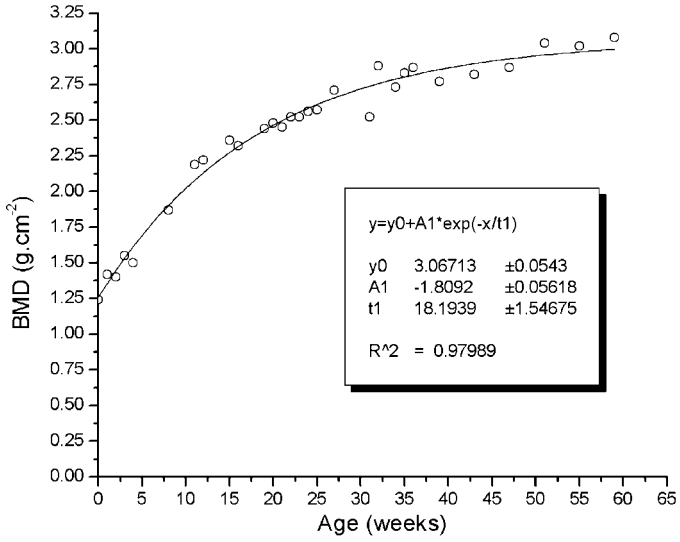

Figure 7. The graph shows the BMD values measured *in vivo* and *in situ* during the first year of life of three Quarter Horse foals. Each value in the graph is the mean value of four measurements made during each of the examinations.

standard deviations are very similar, which gives that the experiment has a reproducibility of 5.5% and a repeatability of 4.1%

A common behaviour is noticeable in the BMD levels of all three horses. This was expected since the foals belonged to the same breeding farm, were born after a normal gestational period (average 345 days), were descended from the same stallion, were kept and raised together receiving the same feeding and had similar growth patterns. The average of the BMD values measured in the three horses is plotted in the graph shown in figure 7.

The short time necessary for a complete bone scan made it possible to examine even newborn foals of less than 24 h of age, even those that still showed some instability while standing, requiring only physical restraint and without the need for tranquillization/sedation.

The results show the effect of age on the development of the BMD of foals in an exponential manner during their first year of life. As there are no publications in the literature of BMD data obtained with gadolinium DPA *in vivo* in foals up to one year of age, comparison of the BMD values of this study with others, that used different techniques, is difficult. Nevertheless, the exponential increase of the BMD with age agrees very well with data also shown by Hoffman *et al* (1999), who obtained BMD data according to age and body weight from foals using radiographic photo-densitometry. In that paper, however, a polynomial function was used to express the behaviour of the BMD curve. The exponential regression seems more appropriate to the development of the BMD during the first year of life since the BMD continues to increase to its maximum values until 4 to 7 years of age (El Shorafa *et al* 1979, Tomioka *et al* 1985, Jeffcott *et al* 1986, Lawrence *et al* 1994), after which it decreases slightly and another mathematical approach would be required.

4. Conclusions

The results obtained with the phantom and the *in vitro* tests demonstrated that, for an acquisition time of 6 s, the prototype is capable of measuring the BMD with an accuracy and precision of,

approximately, 10.5% and 5.3%, respectively. The *in vivo* experiment demonstrated that the reproducibility and repeatability was 5.5% and 4.1%, respectively, for the BMD ranging from 1.24 to 3.08 g cm^{-2}. Other authors mentioned an accuracy and precision of 2% (Cameron and Sorenson 1963, Sorenson and Cameron 1967, Cameron *et al* 1968), but those are works performed *in vitro* and without limiting the time acquisition. Jeffcott *et al* (1986), for instance, had practical difficulties keeping the horse absolutely still for the 90 s required by their system to collect the data. The 6 s scanning period was established after many experiments to find the average time a horse stands still without moving.

The results obtained *in vivo* and *in situ* demonstrated that the bienergetic absorptiometry technique is adequate to determine the BMD in large animals on a breeding farm. No related works with detailed results for the first year of life of horses, using a DPA technique with gadolinium source, were found in the literature to compare. Nevertheless, the measured values presented in this paper are coherent with those values (for adult horses from 2.857 to 3.137 g cm^{-2}) measured at irregular intervals and published by other authors (Tomioka *et al* 1985, Hoffman *et al* 1999).

In table 4, the low value of the standard deviation of the four measurements performed in each horse is noticeable. Thus it is reasonable to assume that two sets of data are enough to derive the BMD, i.e., only one cycle of movement would be necessary.

The BMD study of the equine third metacarpal bone, using gadolinium dual photon absorptiometry, produced new data that have not been available previously. The developed prototype has the ability to derive and follow the BMD levels of horses *in vivo* and *in situ* and to track its behaviour. Based on such data veterinarians and horse breeders may improve the animal's performance by optimizing feeding and training programmes. Even though the gadolinium dual photon absorptiometry technique is able to derive the BMD *in vivo* and *in situ* the main drawbacks of the technique are the costs and the limited lifetime of the gadolinium source.

Acknowledgment

This study was financially supported by CNPq, Brazil (National Scientific and Technological Development Council).

References

Batista E V 2000 Desenvolvimento de um Sistema de Tomografia Computadorizada Aplicado a Ensaios Não Destrutivos *Dissertação de Mestrado* Programa de Pós-Graduação em Engenharia Elétrica e Informática Industrial CPGEI/CEFET-PR Curitiba PR, Brasil

Bell R A, Nielsen B D, Waite K, Rosenstein D and Orth M 2001 Daily access to pasture turnout prevents loss of mineral in the third metacarpus of Arabian weanlings *J. Anim. Sci.* **79** 1142–50

Buckingham S H W and Jeffcott L B 1991 Osteopenic effects of forelimb immobilisation in horses *Vet. Rec.* **128** 370–3

Bushong S 1993 *Radiological Science for Technologists* (St Louis, MO: Mosby-Year Book)

Cameron J R, Mazess R B and Sorenson J A 1968 Precision and accuracy of bone mineral determination by direct photon absorptiometry *Invest. Radiol.* **3** 141

Cameron J R and Sorenson J A 1963 Measurement of bone mineral *in vivo*: an improved method *Science* **142** 230–42

El Shorafa W M, Feaster J P and Ott E A 1979 Horse metacarpal bone: age ash content, cortical area and failure stress interrelationships *J. Anim. Sci.* **49** 979–82

Gong J K, Arnold J S and Cohn S H 1964 The density of organic and volatile and non-volatile inorganic components of bone *Anat. Rec.* **149** 319–24

Grier S J, Turner A S and Alvis M R 1996 The use of dual-energy x-ray absorptiometry in animals *Invest. Radiol.* **31** 50

Hoffman RM, Lawrence L A, Kronfeld D S, Cooper W L, Sklan D J, Dascanio J J and Harris P A 1999 Dietary carbohydrates and fat influence radiographic bone mineral content of growing foals *J. Anim. Sci.* **77** 3330–8

Hubbell J H and Seltzer S M 1995 Tables of x-ray mass attenuation coefficients and mass energy-absorption coefficients 1 keV to 20 MeV for elements $Z = 1$ to 92 and 48 additional substances of dosimetric interest *US Department of Commerce, Technology Administration, National Institute of Standards and Technology, Physics Laboratory, Ionizing Radiation Division*

Jeffcott L B, Buckingham S H W, McCarthy R N, Cleeland J C, Scotti E and McCartney R N 1988 Non-invasive measurement of bone: a review of clinical and research applications in the horse *Equine Vet. J. Suppl.* **6** 71

Jeffcott L B, McCartney R N and Speirs V C 1986 Single photon absorptiometry for the measurement of bone mineral content in horses *Vet. Rec.* **118** 499–505

Krølner B and Nielsen S P 1985 Measurement of bone mineral content (BMD) of the lumbar spine: I. Theory and application of a new two-dimensional dual-photon attenuation method *Scand. J. Clin. Lab. Invest.* **40** 653–63

Lawrence L A, Ott E A, Miller G J, Poulus P W, Piotrowski G and Asquith R L 1994 The mechanical properties of equine third metacarpals as affected by age *J. Anim. Sci.* **72** 2617–23

McClure S R, Glickman L T, Glickman N and Weaver C M 2001 Evaluation of dual energy x-ray absorptiometry for *in situ* measurement of bone mineral density of equine metacarpi *Am. J. Vet. Res.* **62** 752–6

Nielsen B D, Potter G D, Morris E L, Odom T W, Senor D M, Reynolds J A, Smith W B and Martin M T 1997 Changes in third metacarpal bone and frequency of bone injuries in young quarter horses during race training—Observations and theoretical considerations *J. Equine Vet. Sci.* **17** 541–9

Njeh C F, Fuerst T, Hans D, Blake G M and Genant H K 1999 Radiation exposure in bone mineral density assessment *Appl. Radiat. Isot.* **50** 215–36

O'Callaghan M W 1991 Future diagnostic methods *Equine Pract.* **7** 467

Ostlere S J and Gold R H 1991 Osteoporosis and bone density measurement methods *Clin. Orthop. Rel. Res.* **271** 149–63

Piotrowski G, Sullivan M and Colahan P T 1983 Geometric properties of equine metacarpi *J. Biomech.* **16** 129

Porr C A, Ott E A, Johnson E L and Madison J B 1997 Bone mineral in young thoroughbred horses is affected by training *Equine Pract.* **19** 28–31

Scotti E and Jeffcott L B 1988 The hock as a potential site for non-invasive bone measurement *Equine Vet. J. Suppl.* **6** 93

Siemon N J, Moodie E W and Robertson D F 1974 The determination of bone density by radiation absorption *Calcif. Tissue Res.* **15** 189

Sorenson J A and Cameron J R 1967 A reliable *in vivo* measurement of bone-mineral content *J. Bone Joint Surg.* **49A** 481–97

Tomioka Y, Kaneko M, Oikawa M, Kanemaru T, Yoshihara T and Wada R 1985 Bone mineral content of metacarpus in racehorses by photon absorption technique: *in vitro* measurement *Bull. Equine Res. Inst.* **22** 22

Willard H H, Merritt L L Jr, Dean J A and Settle F A Jr 1988 *Instrumental Methods of Analysis* 7th edn (Belmont, CA: Wadsworth Publishing)